EUROFUSION WPMST1-CP(16) 15220

M Garcia-Munoz et al.

The role of plasma response on fast-ion losses induced by applied 3D fields in the ASDEX Upgrade and DIII-D tokamaks

Preprint of Paper to be submitted for publication in
Proceedings of 26th IAEA Fusion Energy Conference

This work has been carried out within the framework of the EUROfusion Consortium and has received funding from the Euratom research and training programme 2014-2018 under grant agreement No 633053. The views and opinions expressed herein do not necessarily reflect those of the European Commission.

The role of plasma response on fast-ion losses induced by edge 3D fields in the ASDEX Upgrade and DIII-D tokamaks

M. Garcia-Munoz[(1)], J. Galdon[(1)], L. Sanchis-Sanchez[(1)], X. Chen[(2)], M. C. Dunne[(3)], N. M. Ferraro[(2)], J. Hanson[(2)], W. W. Heidbrink[(4)], G. Kramer[(5)], Y. Q. Liu[(6)], M. Nocente[(7)], D. C. Pace[(2)], C. Paz-Soldan[(2)], M. Rodriguez-Ramos[(1)], D. Ryan[(6)], A. Snicker[(3)], W. Suttrop[(3)], M. A. Van Zeeland[(2)], and the ASDEX Upgrade, DIII-D and EUROfusion MST1 Teams

[(1)] FAMN Department, Faculty of Physics, University of Seville, 41012 Seville, Spain
[(2)] General Atomics, PO Box 85608 San Diego, California 92186-5608, USA
[(3)] Max-Planck-Institut für Plasmaphysik, D-85748, Germany
[(4)] University of California at Irvine, Irvine, California 92697, USA
[(5)] Princeton Plasma Physics Laboratory, PO Box 451, Princeton, NJ 08543-0451, USA
[(6)] CCFE, Culham Science Centre, Abingdon, OX14 3DB, UK
[(7)] Dipartimento di Fisica 'G. Occhialini', Universita degli Studi di Milano-Bicocca, Piazza della Scienza 3, 20126, Milano, Italy

Email: Manuel.Garcia-Munoz@ipp.mpg.de

Abstract. A joint experimental effort on the DIII-D and ASDEX Upgrade (AUG) tokamaks shows that the fast-ion confinement is extremely sensitive to the poloidal spectra of the externally applied resonant magnetic perturbations (RMP) commonly used to mitigate ELMs. The plasma response, and ultimate internal magnetic perturbation, depends strongly on the RMP poloidal spectra, and this determines the observed impact on the fast-ions. The fast-ion response to the externally applied RMPs is measured in both devices by means of scintillator based Fast-Ion Loss Detectors (FILD) [1] located at different positions. The effect of the plasma response on the poloidal spectra of the total magnetic perturbation, and its impact on fast-ion losses is studied by varying the relative phase between the upper and lower sets of RMP coils existing in both devices. In DIII-D, a large perturbation is observed on a magnetic probe for 0º relative phasing, while a much smaller response is measured for 240º phasing. These changes are caused by changes in the plasma response associated with coupling to resonant and non-resonant internal kinks. When the RMP is applied, the oscillating n=1 fast-ion loss signal more than doubles for the phasing that couples to the resonant internal kink. Companion experiments conducted at AUG similarly show that fast-ion losses increase with plasma response, with changes in the poloidal spectra of the RMP having a strong effect on the plasma response and, consequently, on the fast-ion losses. As in DIII-D, the maximum measured fast-ion losses appear when the coupling to the internal kink is maximized. The fast-ion behaviour in the resulting 3D fields have been simulated with the SPIRAL and ASCOT codes using both vacuum fields and the plasma response calculated with the M3D-C1 and MARS-F MHD codes. Simulations reproduce the strong correlation of the fast-ion transport with the poloidal spectra of the applied RMPs. The maximum transport happens in a resonant layer of ~ 5 cm within the separatrix. This fast-ion resonance with the resulting 3D fields can lead to both an enhancement of the fast-ion loss but also to an improvement of the fast-ion confinement opening new avenues for the control of the fast-ion population as well as for the optimization of the externally applied RMPs for ELM suppression.

1. Introduction.

Edge localized modes (ELMs) are inherent to high confinement regimes in tokamak plasmas. The energy and particle release following large ELM crashes are thought to be intolerable in future fusion devices such as ITER; consequently, extensive efforts are dedicated to the development of reliable mitigation techniques that are compatible with high confinement regimes. Among others, externally applied resonant magnetic perturbations (RMPs) are one of the most promising techniques [2–5]. Recent observations have highlighted the important role that the plasma response to the externally applied 3D fields plays in the ELM suppression mechanism. Indeed, a significant kink response seems to be necessary to explain the ELM suppression and density pump-out observed in DIII-D experiments for a certain RMP poloidal spectrum [6, 7]. The impact that the RMP poloidal spectrum, and associated plasma response, has on the fast-ion confinement still needs to be assessed. This is of special importance for future burning plasmas with a large content of MeV-ions with relatively long slowing-down times. Numerical simulations of fast-ion losses induced by ELM mitigation coils in ITER [8] have shown that, under certain conditions, up to 20% of the neutral beam injection (NBI) power can be lost due to the 3D fields created by the ELM mitigation coils. First experiments at AUG and DIII-D have shown that under certain conditions externally applied RMPs can cause a significant degradation of the fast-ion confinement [9, 10].

In this paper, measurements of fast-ion losses as a function of the RMP coils configuration, and subsequent plasma response, obtained in the DIII-D and AUG tokamaks are presented. The experiments discussed here have been carried out in low q_{95} and collisionallity, ELMy H-mode plasmas. The poloidal spectra of the applied RMP has been modified by varying the relative phase between the upper and lower sets of RMP coils. In DIII-D, the plasma response to the applied RMP poloidal spectra has been studied as a function of the plasma pressure. In both devices, the measured fast-ion losses depend strongly on the plasma response to the applied 3D fields. While in DIII-D, a 15% modulation of the fast-ion losses with the applied 3D fields is observed over the entire 360º scan of the n=2 RMP poloidal spectra, the fast-ion losses in AUG are observed only with a certain poloidal spectra of the applied n=2 RMP. A clear correlation between the measured fast-ion losses and the plasma response is observed in both devices though with a clear phase shift that can be up to 50º. In both devices, the escaping ions are on banana orbits that explore the entire plasma pedestal. Full orbit simulations carried out with the SPIRAL [11] and

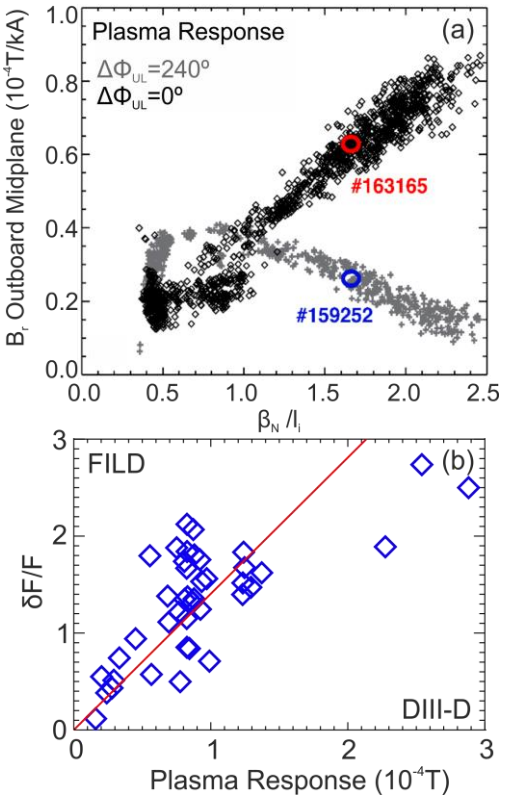

Fig. 1. (a) Plasma response to n=1 RMPs measured at the outboard midplane as function of β_N/L_i. (b) Amplitude of modulated fast-ion losses versus amplitude of plasma response.

ASCOT [12] codes using 3D fields calculated with the MHD M3D-C1 [13] and MARS-F [14] codes reproduce the strong correlation between the fast-ion losses and the applied RMP poloidal spectra. Calculations of the change in the fast-ion toroidal canonical angular momentum due to the applied 3D fields, including plasma response, show that the maximum transport is localized within a resonant layer of approximately 5 cm at the very edge of the plasma while internal resonances appear for certain coil configurations that maximizes the kink response. Section 2 is devoted to the main observations and modelling results at DIII-D, while section 3 is dedicated to the companion results at AUG. Some conclusions are finally given in section 4.

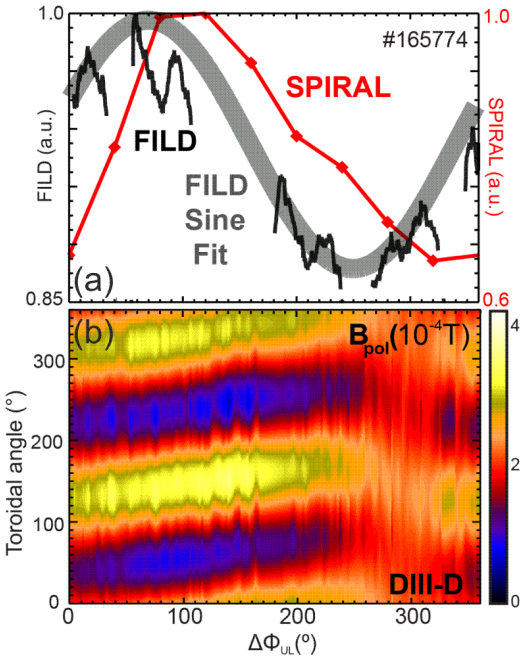

Fig.2. DIII-D #165774.
(a) Measured fast-ion losses at FILD2 (thin black line), sinusoidal fit to FILD signal (grey) and simulated FILD signal with SPIRAL and M3D-C1 fields (red). (b) Measured plasma response at the outboard midplane.

2. Fast-ion response to externally applied RMPs in DIII-D.

In DIII-D, two sets of experiments have been carried out. The plasma response to the external RMP and associated fast-ion losses has been studied as a function of β_N for two different coils phasings ($\Delta\Phi_{UL}$) using an n=1 rigid rotation in a large data base of discharges. In a separate experiment, the impact that the poloidal spectra has on the plasma response and subsequent fast-ion loss has been studied in a single experiment with a continuous differential phase scan of an n=2 RMP. In Fig. 1.-(a), the plasma response to a n=1 RMP measured at the outboard midplane is shown as a function of the normalized β_N/l_i for two different $\Delta\Phi_{UL}$. The plasma response can be up to a factor of 4 larger for the coils configuration, $\Delta\Phi_{UL}$=0, that couples the external RMP to the internal kink increasing linearly with β_N/l_i. The amplitude of the modulated fast-ion losses with the rotating n=1 RMP shows a clear linear dependency with the measured plasma response to the applied external fields for relatively weak plasma responses (below 1.5 10^{-4} T), see Fig. 1-(b).

A detailed study of the plasma and fast-ion response to the poloidal spectra of the externally applied 3D fields has been carried out by varying $\Delta\Phi_{UL}$ continuously in a discharge with an n=2 RMP and keeping all other relevant plasma parameters constant. Fig. 2 shows the measured fast-ion losses at (a) FILD2 and (b) plasma response at the outboard midplane as function of $\Delta\Phi_{UL}$. A 15% modulation with $\Delta\Phi_{UL}$ in the FILD signal can be clearly observed. One can also observed a phase shift of approximately 50º between the peak fast-ion losses in Fig. 2.-(a) and the maximum plasma response in Fig. 2.-(b). The large fast-ion orbit drifts could be responsible for this phase shift between the maxima in the measured fast-ion losses and plasma response. The velocity-space of the escaping ions measured by FILD identifies unequivocally the orbits of the ions that are most affected by the perturbation fields. In Fig. 3.-(a), the energy and pitch-angle of the escaping ions

measured by FILD2 are shown. The losses appear at a well-defined pitch-angle, ~55-60º, but with a broad energy distribution between 30 and 80 keV that corresponds to banana orbits that explore the entire pedestal, see Fig. 3.-(b).

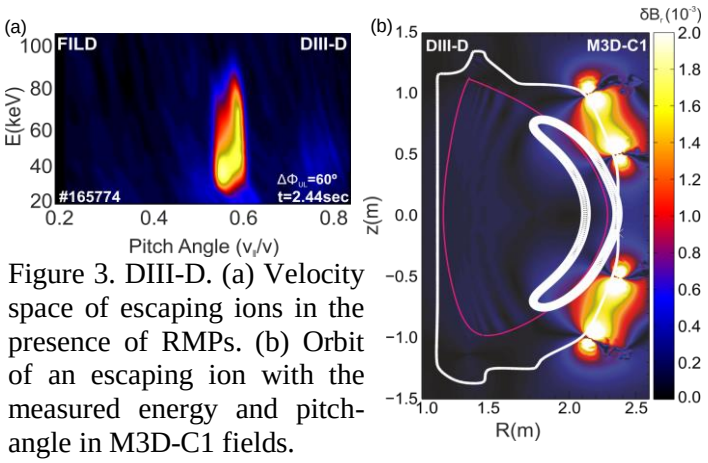

Figure 3. DIII-D. (a) Velocity space of escaping ions in the presence of RMPs. (b) Orbit of an escaping ion with the measured energy and pitch-angle in M3D-C1 fields.

SPIRAL simulations of the fast-ion behavior in the resulting 3D fields have been carried out using linear, two-fluid, and resistive M3D-C1 calculations of the plasma response. The fast-ion population created by the 30L beam has been modeled by a distribution of ions with the pitch-angle defined by the 30L beam injection geometry and the injection energies. The red curve in Fig. 2.-(a) shows the fast-ion losses simulated with SPIRAL in M3D-C1 fields for the different $\Delta\Phi_{UL}$. The modulation in the simulated losses is in phase with the measured plasma response but ~50º off with respect to the measured fast-ion losses.

Calculations of the variation of the fast-ion canonical angular momentum (δP_Φ) as a function of $\Delta\Phi_{UL}$ in M3D-C1 fields show that the first orbit losses suffer the maximum δP_Φ for $\Delta\Phi_{UL}$=180º, see Fig. 4.-(a), while the delayed losses (after a few bounces), Fig. 4.-(b), suffer the maximum δP_Φ for $\Delta\Phi_{UL}$=80º which is in agreement with the measured losses, see Fig. 2-(a). Fig. 4.-(c) shows that the confined ions suffer the maximum δP_Φ, at a different $\Delta\Phi_{UL}$ suggesting a dependency of the fast-ion transport radial profile on the poloidal spectra of the applied 3D fields. An additional spread in δP_Φ due to collisions is also visible.

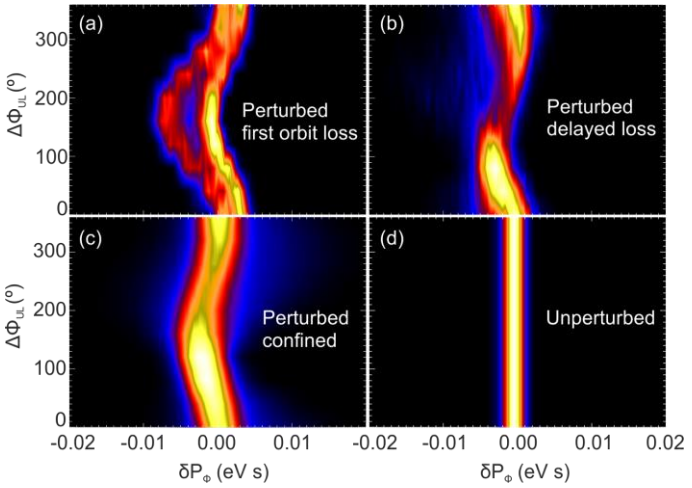

Figure 4. Perturbation of the fast-ion canonical angular momentum, δP_Φ, due to collisions and the applied 3D fields for (a) first orbit losses, (b) delayed losses, (c) confined ions and (d) reference case without 3D fields.

3. Fast-ion response to externally applied RMPs in AUG.

A continuous differential phase scan has been carried out in an AUG ELMy H-mode plasma with relatively high β_N and low collisionality and q_{95} to study the fast-ion and plasma response to the applied n=2 RMP poloidal spectra.

As in DIII-D, the current flowing through the lower set of coils were kept constant while the current flowing through the upper set of coils was modulated as Fig. 5.-(d) shows. This modulation results in a complete $\Delta\Phi_{UL}$ scan in 0.5 sec. Fig. 5.-(a) shows the fast-ion losses measured with FILD2 over three periods of the RMP poloidal spectra scan. The fast-ion losses are always measured at the same relative phase, $\Delta\Phi_{UL,}$ in all three scans while the density pump-out, Fig. 5.-(b), and ELM mitigation, Fig. 5-(c), is clearly observed as soon as the coils are energized. The velocity-space of the escaping ions, Fig. 6.-(a), measured with FILD2 indicate that most of the losses appear at a pitch-angle of ~55º and energies of ~ 45 keV while other lower pitch-angles are also visible at somewhat higher energies. As in the DIII-D case, the dominant losses correspond to fast-ions on trapped orbits that explore the entire pedestal, see Fig.6.-(b), though some escaping ions on passing orbits with pitch-angles between 30º and 40º are also observed. The perturbed 3D fields are calculated using the linear one-fluid, resistive MHD MARS-F code for the entire scan of the poloidal spectra for a single toroidal mode number n=2. The effect that other toroidal harmonics could have on the overall plasma response and subsequent losses is not considered in the plasma response simulations. Fig. 6.-(b) shows the entire δB_r (vacuum + plasma response) on a poloidal cross-section for $\Delta\Phi_{UL}$=180º. MARS-F predicts a significant shielding of the external n=2 field line resonant 3D fields for the entire $\Delta\Phi_{UL}$ scan. The maximum shielding over the entire plasma appears at $\Delta\Phi_{UL}$=0º while a strong global kink-peeling response is observed at $\Delta\Phi_{UL}$=180º. Fig. 7 shows the plasma displacement perpendicular to the magnetic flux surfaces, including the plasmas response for $\Delta\Phi_{UL}$=0º and $\Delta\Phi_{UL}$=180º. At $\Delta\Phi_{UL}$=0º, Fig. 7.-(a) and (c), a clear and well localized peeling response is observed while at $\Delta\Phi_{UL}$=180º, Fig. 7-(b) and (d), a maximum displacement of ~2.4 mm is observed due to an internal kink response at s~0.65.

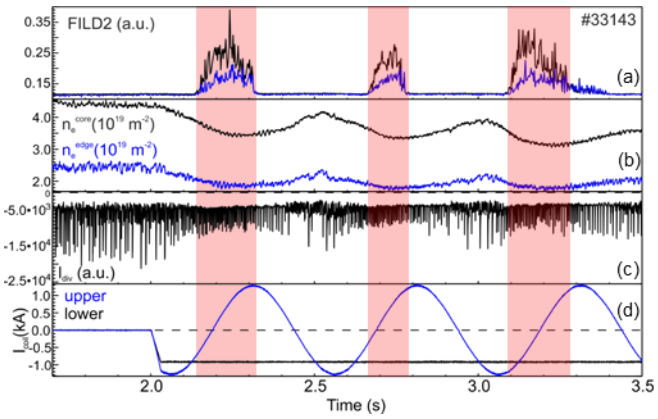

Figure 5. AUG #33143. (a) Fast-ion losses measured with FILD2. (b) Time trace of core (black) and edge (blue) line integrated density. (c) Divertor current as ELM monitor. (d) Time trace of coils current.

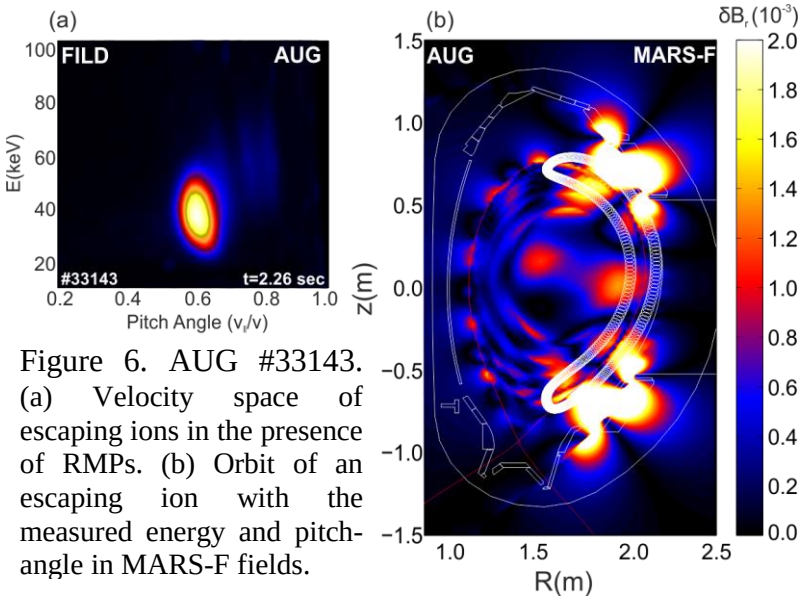

Figure 6. AUG #33143. (a) Velocity space of escaping ions in the presence of RMPs. (b) Orbit of an escaping ion with the measured energy and pitch-angle in MARS-F fields.

Drift orbit simulations have been carried with the ASCOT code and the 3D fields calculated using the vacuum approach as well as the MARS-F plasma response. The fast-ion population has been modeled by a distribution with a well-defined pitch-angle given by the NBI injection geometry and a realistic birth energy distribution. The simulated fast-ion losses show a clear dependency with the poloidal spectra of the applied RMP for both, the vacuum and MARS-F fields. ASCOT predicts significant losses for $\Delta\Phi_{UL}$ between 0º and 180º while for $\Delta\Phi_{UL}$>180º, the global fast-ion losses are strongly reduced. The strong plasma shielding between $\Delta\Phi_{UL}$=0º and $\Delta\Phi_{UL}$~80º lead to a slight reduction of the fast-ion losses with respect to the losses obtained using vacuum fields. Fig. 8.-(a) shows the total fast-ion losses simulated with ASCOT using n=2 MARS-F fields (blue), n=2 vacuum fields (black) as well as the 3D fields arising from the complete RMP spectrum calculated in vacuum (red). A 100% modulation of the losses is observed in the $\Delta\Phi_{UL}$ scan for all fields. The maximum losses appear with the vacuum fields that contain the entire RMP spectra (mainly n=2 and n=6) for $\Delta\Phi_{UL}$=40-50º. The fast-ion losses induced by solely the n=2 fields are up to 20% lower than those obtained using the entire RMP spectrum. The plasma response to the applied n=2 fields leads to a slight reduction of the losses for $\Delta\Phi_{UL}$=40º due to a significant shielding of the external perturbation, see Fig. 7-(a) and (c). A slight enhancement of the losses is, on the contrary, observed for $\Delta\Phi_{UL}$=160º due to a strong internal kink response, see Fig. 7-(b) and (d). The simulated losses at FILD reproduce the strong dependency of the measured fast-ion losses with the applied RMP poloidal

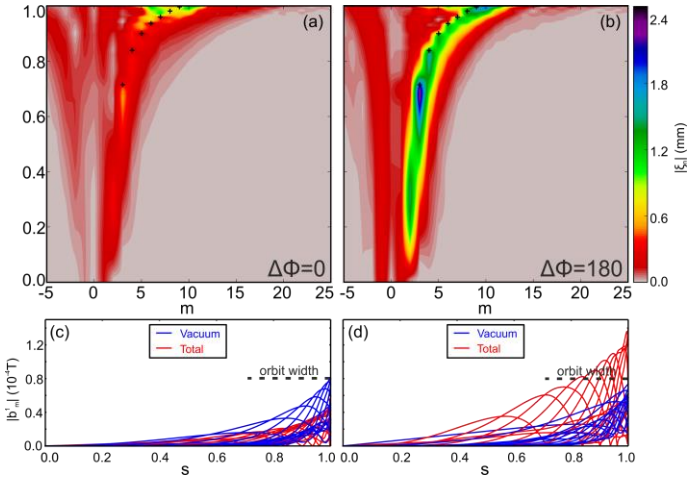

Figure 7. Plasma response calculated with MARS-F. Spectrogram of displacement perpendicular to flux surface for (a) $\Delta\Phi_{UL}$=0º and (b) $\Delta\Phi_{UL}$=180º. Radial profile of magnetic perturbation for (c) $\Delta\Phi_{UL}$=0º and (d) $\Delta\Phi_{UL}$=180º. The orbit width of a typical escaping ion is depicted with a horizontal dashed line.

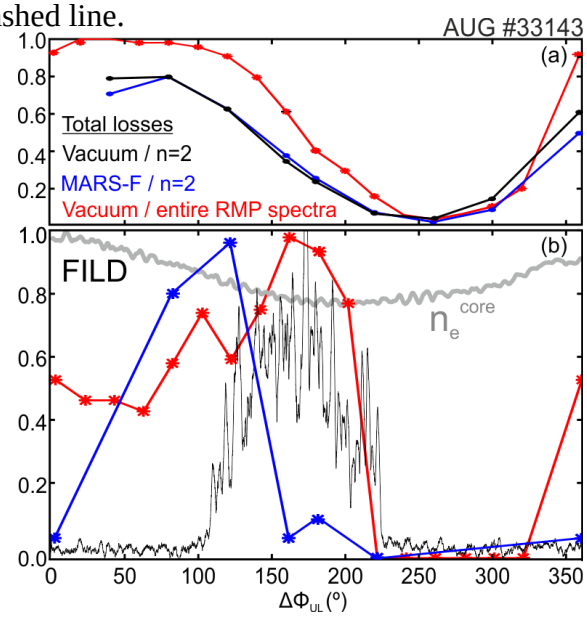

Figure 8. (a) Total losses simulated with ASCOT using n=2 vacuum fields (black), n=2 MARS-F fields (blue) and the entire RMP spectra calculated in vacuum (red). (b) Normalized fast-ion losses measured with FILD2 (black), core density (grey) and expected losses simulated with ASCOT using MARS-F fields (blue) and the entire RMP spectra calculated in vacuum (red).

spectra for both the n=2 MARS-F fields and the vacuum fields of the entire RMP spectrum, showing a well-defined maximum, see Fig. 8.-(b). In agreement with FILD measurements, the maximum in the simulated losses appear for $\Delta\Phi_{UL}$=180º for the vacuum fields of the entire RMP spectrum while the maximum in the losses for the n=2 MARS-F fields appear for $\Delta\Phi_{UL}$=120º. As in DIII-D, a phase-shift of ~50-60º in $\Delta\Phi_{UL}$ is obtained between the maximum in the measured and simulated fast-losses indicating that the toroidal harmonics of the applied n=2 3D fields may play an important role in the measured fast-ion losses. The vacuum fields of the entire RMP spectrum cause, however, losses at FILD for $\Delta\Phi_{UL}$=0-100º that are not observed in the experiments suggesting that the plasma response to the entire RMP spectrum should be included to reproduce more accurately the experimental observations.

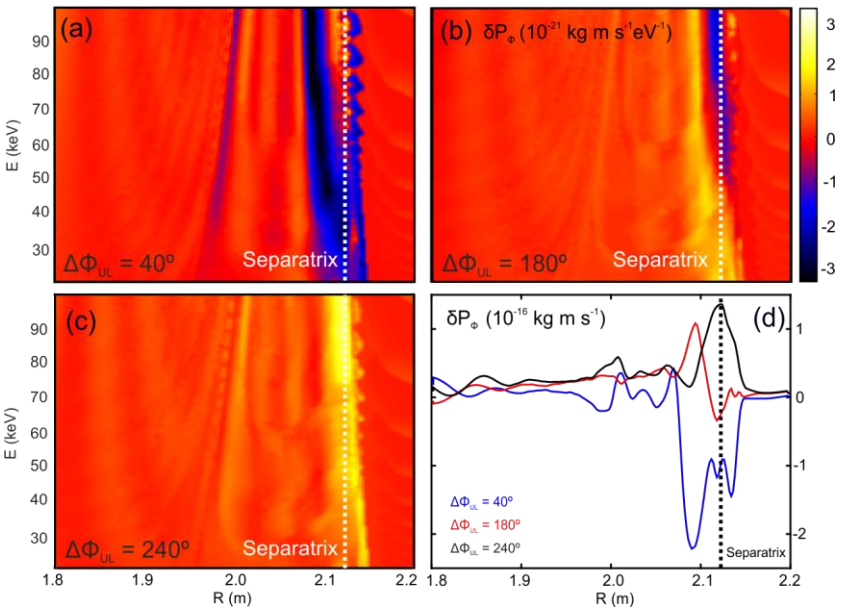

Figure 9. AUG. ASCOT vacuum. Variation of the fast-ion canonical angular momentum as function of fast-ion energy and plasma major radius for different coils differential phases, (a)-(c), and (d) integrated for all energies.

In order to understand the transport mechanism underlying the observed RMP induced fast-ion losses, the radial variation of the fast-ion canonical angular momentum, δP_Φ, has been computed for the fast-ion population considered here and the entire $\Delta\Phi_{UL}$ scan. Simulations show that the fast-ion transport induced by the external 3D fields is highly dependent on the applied RMP poloidal spectra, and the particle energy and location for the beam ions considered here, e.g. dominant pitch-angle given by the beam injection geometry. Fig. 9 shows the fast-ion δP_Φ induced by the applied 3D fields on the simulated ensemble of particles for $\Delta\Phi_{UL}$=40º, (a), $\Delta\Phi_{UL}$=180º, (b) and $\Delta\Phi_{UL}$=240º, (c). An outwards particle transport corresponds here to a δP_Φ<0. Depending on the poloidal spectrum of the applied RMP, an outwards or inwards fast-ion transport can be obtained. The direction of the local transport depends strongly on the fast-ion energy, being possible to have, for instance, an outwards transport of particles, with energies above a certain value, and an inwards transport of particles with energies below that value, ~50 keV for $\Delta\Phi_{UL}$=180º, see Fig. 9.-(b). For the case under study, a $\Delta\Phi_{UL}$=40º induces an outwards fast-ion transport in the entire energy spectra as Fig. 9.-(a) shows, while the RMP with $\Delta\Phi_{UL}$=240º improves the fast-ion confinement. In agreement with the total simulated losses and FILD measurements, no losses are either expected or observed for $\Delta\Phi_{UL}$=240º, see Fig. 8. The rather vertical structures observed in Fig. 9-(a)-(c) within ~5 cm around the separatrix correspond to rational $\omega_{pol}/\omega_{prec}$ fast-ion resonances with the applied 3D fields. Here ω_{pol} is the poloidal

transit frequency and ω_{prec} the toroidal transit frequency. A δP_Φ radial profile, integrated over the entire energy spectra, shows that the maximum fast-ion transport is localized within ~5cm (~fast-ion gyroradius) around the separatrix for all poloidal spectra of the n=2 RMP considered here, see Fig. 9-(d). The plasma shielding / amplification of the local magnetic perturbation can, however, lead to a modification of this transport profile.

4. Conclusions.

In AUG and DIII-D, recent experiments show that the fast-ion losses are extremely sensitive to the poloidal spectra of the applied RMPs. The measured fast-ion losses depends linearly on the measured plasma response for weak fields, this linear dependency is, however, distorted for a strong plasma response. The results presented here suggest that toroidal harmonics of the main applied RMP may play an important role in the observed fast-ion losses. The plasma response to the entire RMP spectrum should be, consequently, taken into account. Indeed, simulations show a clear impact of the plasma shielding and peeling-kink amplification on the total fast-ion losses. Depending on the applied RMP poloidal spectra, the 3D fields can couple to the internal kink causing an enhancement of the fast-ion losses. The maximum fast-ion transport due to the applied 3D fields happens in a resonant layer of ~ 5 cm within the separatrix. This fast-ion resonance with the resulting 3D fields can lead to both an enhancement of the fast-ion loss but also to an improvement of the fast-ion confinement opening new avenues for the control of the fast-ion population as well as for the optimization of the externally applied RMPs for ELM suppression.

Acknowledgements

This work has been carried out within the framework of the EUROfusion Consortium and has received funding from the Euratom research and training programme 2014-2018 under grant agreement No 633053. The views and opinions expressed herein do not necessarily reflect those of the European Commission. This work supported by the US Department of Energy, Office of Science, Office of Fusion Energy Sciences, using the DIII-D National Fusion Facility, a DOE Office of Science user facility, under Award DE-FC02-04ER54698. DIII-D data shown in this paper can be obtained by following the links at https://fusion.gat.com/global/D3D_DMP. This research was also supported by the Spanish Ministry of Economy and Competitiveness (RYC-2011-09152 and ENE2012-31087) and a Marie Curie FP7 Integration Grant (PCIG11-GA-2012-321455).

References

[1] M. Garcia-Munoz et al., Rev. Sci. Instrum. **80**, 053503 (2009)
[2] T. C. Hender et al., Nucl. Fusion **32,** 2091 (1992)
[3] T. E. Evans et al., Phys. Rev. Lett. **92,** 235003 (2004)
[4] Y. Liang et al., Phys. Rev. Lett. **98,** 265004 (2007)
[5] W. Suttrop et al., Phys. Rev. Lett. **106,** 225004 (2011)
[6] C. Paz-Soldan et al., Phys. Rev. Lett. **114**, 105001 (2015)
[7] Y. Q. Liu et al., Nucl. Fusion **51**, 083002 (2011)
[8] K. Shinohara et al., Nucl. Fusion **51,** 063028 (2011)
[9] M. Garcia-Munoz et al., Plasma Phys. Control. Fusion **55,** 124014 (2013)
[10] M. A. Van Zeeland et al., Plasma Phys. Control. Fusion **56**, 015009 (2014)
[11] G. Kramer et al., Plasma Phys. Control. Fusion **55**, 025013 (2013)
[12] A. Snicker et al., Nucl. Fusion **53**, 093028 (2013)
[13] N. M. Ferraro, Phys. Plasmas **19,** 056105 (2012)
[14] Y. Q. Liu et al., Phys. Plasmas **7,** 3681 (2000)